NASA-CR-201025

DEPARTMENT OF AEROSPACE ENGINEERING
COLLEGE OF ENGINEERING & TECHNOLOGY
OLD DOMINION UNIVERSITY
NORFOLK, VIRGINIA 23529

ASSUMED--STRESS HYBRID ELEMENTS WITH DRILLING DEGREES OF FREEDOM FOR NONLINEAR ANALYSIS OF COMPOSITE STRUCTURES

By

Dr. Norman F. Knight, Jr., Principal Investigator

Final Report
For the period ended December 31, 1995

Prepared for
National Aeronautics and Space Administration
Langley Research Center
Hampton, VA 23681-0001

Under
Research Grant NAG-1-1505
R. Keith Norwood, Technical Monitor
SD-Computational Mechanics Branch

Submitted by the
Old Dominion University Research Foundation
P.O. Box 6369
Norfolk, VA 23508-0369

June 1996

Assumed–Stress Hybrid Elements with Drilling Degrees of Freedom for Nonlinear Analysis of Composite Structures – Final Report for NAG–1–1505 –

Submitted to:

Computational Mechanics Branch
Structures Division
NASA Langley Research Center
Hampton, Virginia 23681–0001

by the

Department of Aerospace Engineering
College of Engineering and Technology
Old Dominion University

Principal Investigator:

N. F. Knight, Jr, D.Sc.
Associate Professor of Aerospace Engineering
Old Dominion University, Norfolk, VA 23529–0247
Telephone No. (804) 683–4265
E–mail: knight@aero.odu.edu

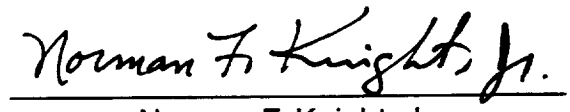

Norman F. Knight, Jr.
Principal Investigator

May 1996

TABLE OF CONTENTS

ASSUMED–STRESS HYBRID ELEMENTS WITH DRILLING DEGREES OF FREEDOM FOR NONLINEAR ANALYSIS OF COMPOSITE STRUCTURES – FINAL REPORT FOR NAG–1–1505 –

Norman F. Knight, Jr.
Department of Aerospace Engineering
Old Dominion University
Norfolk, VA 23529–0247

SUMMARY

The goal of this research project is to develop assumed–stress hybrid elements with rotational degrees of freedom for analyzing composite structures. During the first year of the three–year activity, the effort was directed to further assess the AQ4 shell element and its extensions to buckling and free vibration problems. In addition, the development of a compatible 2–node beam element was to be accomplished. The extensions and new developments were implemented in the Computational Structural Mechanics Testbed COMET. An assessment was performed to verify the implementation and to assess the performance of these elements in terms of accuracy. During the second and third years, extensions to geometrically nonlinear problems were developed and tested. This effort involved working with the nonlinear solution strategy as well as the nonlinear formulation for the elements.

This research has resulted in the development and implementation of two additional element processors (ES22 for the beam element and ES24 for the shell elements) in COMET. The software was developed using a SUN workstation and has been ported to the NASA Langley Convex named blackbird. Both element processors are now part of the baseline version of COMET.

The initial grant (NAG–1–1374) had a period of performance of January 10, 1992 to January 14, 1993 with an approved no–cost extension until May 15, 1993 while the principal investigator was affiliated with Clemson University. Dr. Alexander Tessler was the Contracting Officer's Technical Representative (COTR). In January 1993, the principal investigator moved to Old Dominion University and a new grant activity was established (NAG–1–1505). This grant had a period of performance of April 10, 1993 until May 15, 1996 with an approved no–cost extension until December 31, 1996. Initially, Dr. Tessler remained the COTR for NAG–1–1505; then Mr. Keith Norwood assumed that role. When Mr. Norwood left NASA Langley, Dr. W. Jefferson Stroud became the COTR for a short period and then Dr. Tessler re–assumed that role.

OVERVIEW OF GRANT

NAG–1–1374 (Clemson First Year: 1/10/92 to 5/15/93)	
Grant Objectives	**Grant Accomplishments**
Assess AQ4 formulation, implementation, capabilities	Developed symbolic approach for deriving these elements based on MAPLE; compared computational efforts (1 journal paper); 1 MS on beam element;
Develop compatible beam element	
Develop compatible triangular element	Deferred; told to emphasize beam element first
Demonstrate combined use of elements	Sobel used elements on Grumman panel
Extend to buckling problems	Developed geometric stiffness matrices
Extend to free vibration problems	Developed consistent mass matrices
Extend to geometrically nonlinear problems	Deferred
Utilize GEP in COMET	ES22 (beam element) and ES24 (quad element)
NAG–1–1505 (ODU First Year: 4/16/93 to 5/16/94)	
Grant Objectives	**Grant Accomplishments**
Explore alternative stress fields	1 MS on quad element; 1 journal paper on formulation
Derive diagonal mass coefficients	HZR mass lumping for quad and beam
Assess alternate stress recovery procedures	Stress parameters; differentiating displacement field
Redevelop beam element for GCP formulation	Force/moment resultants in LAUB & GCP different
Develop further test cases for quad element	Skewed plate buckling; cylinder buckling & vibration; pear–shaped cylinder
Develop compatible triangular element	Deferred
Demonstrate combined use of elements	
Supplement for ADR Work (Summer 1993)	
Explore use of ADR on parallel computers	Effective algorithm developed; 4 journal papers, 1 PhD; presentation to CSB in Aug. 1993
Supplement for Interface Element Work (Spring Semester 1994)	
Extend to elements with drilling freedoms	Software changes
Extend to curved 1–D interfaces	1 SDM paper
Assess solvers	Software access
NAG–1–1505 (ODU Second Year: 5/16/94 to 12/31/95)	
Grant Objectives	**Grant Accomplishments**
Review of NL_STATIC_1 in preparation for nonlinear analysis work	Tutorial given to CSB on 1/6/95; problems found with ES6
Extend beam to geometrically nonlinear problems	Develop internal force vector; Demonstrate planar and spatial response prediction; 1 MS; 1 SDM paper; placed 2nd at Mid–Atlantic AIAA student paper competition in April 1995; ES22 documentation
Extend quad to geometrically nonlinear problems	Develop internal force vector; Demonstrated accuracy of low–order corotational approach for problems;
Develop compatible triangular element	Initiated but then deferred due to difficulties encountered with quad element for Raasch problem and with nonlinear problems having high number of halfwaves.
Explore use of interface element to surfaces	Work transferred; separate grant with Aminpour as PI

BACKGROUND

Finite element technology continues to be a major research topic in shell analysis studies. Although the finite element method is well established in the engineering community, several areas of element research are active and new contributions are being made. These research areas are focused on the element formulation, eliminating element sensitivity to mesh distortion, and providing a compatible set of element for modeling aerospace structures. The first element technology research area is associated with the element formulation itself. Generally the formulation is denoted as either C^0 or C^1. Formulations denoted as C^0 include the effects of transverse shear deformation which implies that the out–of–plane deflections and the bending rotations are approximated independently. In a C^0 element, the out–of–plane deflections and the bending rotations may be approximated using the same interpolation or shape functions (e. g., bilinear or biquadratic functions). Formulations denoted as C^1 are based on classical formulations which assume zero transverse shear flexibility. In a C^1 element, the out–of–plane deflections and the bending rotations are generally coupled in that a cubic interpolation is assumed for the out–of–plane deflections (e. g., Hermitian shape functions). In general, C^0 elements are more readily implemented than C^1 elements; however, C^0 elements are also more susceptible to rank deficiencies which may cause element "locking". While reduced integration (either uniform or selective) has been used to alleviate element "locking," it may also introduce spurious modes in the finite element analysis solution. Element formulations also differ in their starting point from the weak–form of the variational statement. For example, formulations based on the principle of minimum potential energy results in displacement–based elements. However, through the use of alternate variational statements (e.g., Hellinger–Reissner principle), assumed stress hybrid formulations can be developed. In a hybrid formulation, the stress field across the element domain is assumed in such a way that the equilibrium equations are satisfied on the interior of the element and the displacement field is assumed only along the element boundaries. Elements based on a hybrid formulation are generally more accurate than displacement–based elements; however, they do pose difficulties in extending these elements to nonlinear problems.

The second element technology research area is associated with eliminating mesh distortion sensitivity. Distorted meshes, where the element shape deviates significantly from a planar square, are common occurrences in most structural analysis problems. These meshes are caused by the complexity of the structural geometry, by the use of mesh transition schemes to reduce the size of the computational problem, and by including nonlinear effects which may transform a regular mesh into a distorted mesh due to large deflections

and rotations. The effect of mesh distortion on shell response predictions has been reported by Stanley et al. (1986), Park and Stanley (1986), and Stanley (1989). Recently new formulations have been emerging which reduce or eliminate the effects of mesh distortion from the element formulation. One such formulation is the assumed natural–coordinate strain or ANS formulation developed by Park and Stanley (1986). Their 9–node ANS quadrilateral shell element has been shown to be nearly insensitive to mesh distortion. However, this element fails the patch test. Another formulation is the 4–node assumed–stress hybrid shell element (AQ4) developed by Aminpour (1990a,b) which uses the same bending displacement field approximations as Tessler and Hughes (1983). The AQ4 element has rotational degrees of freedom that are normal to the element surface or drilling freedoms which are used to improve the inplane displacement field approximations. The AQ4 element has been demonstrated to be accurate, pass both the membrane and bending patch tests, is nearly insensitive to mesh distortion, does not lock, and is invariant with respect to node numbering.

The third element technology research area is associated with providing a compatible set of elements for modeling aerospace structures. Developers of robust shell elements must also be concerned with how the new elements will be used by the structural analysis community. Large–scale complexity applications require a compatible set, or family, of elements for modeling and analysis. This family of elements should be capable of representing both 1–D and 2–D structures and should provide quadrilateral as well as triangular shell elements along with compatible beam elements. Having these elements available, analysts are provided the modeling flexibility needed to represent aerospace structures.

ORIGINAL RESEARCH OBJECTIVES

The specific research objectives initially proposed for this grant were as followed:

- During the first year (9/1/91 to 8/31/92), an independent assessment of the performance of the AQ4 element will be made using test cases involving composite and built–up structures. In addition a 3–node triangular shell element (AQ3) and a 2–node beam element (AQ2) will be developed and implemented in COMET using the GEP. These elements will be compatible with the AQ4 shell element.
- During the second year (9/1/92 to 8/31/93), the formulation of each of these elements will be extended to address buckling problems. Specific test cases will be posed to verify the implementation and the also the robustness of the elements. In addition, the modeling flexibility provided by this family of elements will be demonstrated (i.e., analyze a model which incorporates the AQ2, AQ3, and AQ4 elements.
- During the third year (9/1/93 to 8/31/94), the formulation of each of these elements will be extended to address geometrically nonlinear analyses. Specific test cases will be posed to verify the implementation and the also the robustness of the elements.

However, these objectives were modified early in the first year after discussions with Dr. Jerrold Housner during the first grant review on May 28, 1992. The specific objectives for the first year were to concentrate the effort on the 4–node quadrilateral shell element and the 2–node beam element and provide capabilities for linear stress, buckling and free vibration problems for both elements.

FIRST–YEAR PROGRESS REPORT

The progress made during the first year is divided into two parts. One part deals with the further assessment of the AQ4 shell element and its extensions to linear buckling and free vibration problems. This research was conducted in part by Mr. Govind Rengarajan and resulted in his Master's thesis (Rengarajan, 1993). The second part deals with the development of an AQ4–compatible 2–node beam element with capabilities for linear stress, buckling and free vibration analyses. This research was conducted in part by Mr. Venkateshwar Deshpande and resulted in his Master's thesis (Deshpande, 1993).

Shell Element Research

The work related to the 4–node shell element began with Aminpour's AQ4 element (1990a,b) and implemented in COMET (Stewart, 1989) as element processor ES8/AQ4 using the generic element processor (Stanley and Nour–Omid, 1990). A family of assumed–stress hybrid shell elements was installed as element processor ES24 in COMET. Three areas of research were investigated: (i) use of symbolic computations to accelerate the element computations; (ii) extensions to linear buckling and free vibration analyses; and (iii) use of bubble functions and higher order stress approximations. The basic results for each area will now be summarized.

Use of Symbolic Computations – Assumed–stress hybrid elements are usually associated with higher computational cost due to the fact that a matrix inverse is needed in the evaluation of certain element matrices. For example the element stiffness matrix for the AQ4 shell element is a 24×24 matrix that is computed as followed:

$$[k_e]_{24\times24} = [T_e]^T[H_e]^{-1}[T_e]$$

where

$$[H_e]_{22\times22} = \int_{A_e} [P]^T[D][P]dA$$

$$[T_e]_{22\times24} = \int_{A_e} [P]^T[L][N]dA$$

The matrix $[D]$ is the compliance matrix from the strain–stress relations; the matrix $[L]$ is the linear differential operator matrix from the strain–displacement relations; the matrix $[P]$ is the matrix of stress field approximations; and the matrix $[N]$ is the matrix of displacement field approximations or shape functions. The need to invert the matrix $[H_e]$ for each element and to evaluate two integrals over the area of the element significantly increases the element computation time. Traditionally these operations are performed numerically. That is, Gaussian quadrature is used to evaluate each entry in the matrices $[H_e]$ and $[T_e]$, and then an explicit matrix inverse of $[H_e]$ is computed. In this research, symbolic computations using the MAPLE software system (Char et al., 1991) are used to evaluate the two integrals exactly. Explicit symbolic expressions for $[H_e]$ inverse could not be obtained even when represented as the adjoint and determinant of $[H_e]$. However, since the explicit inverse is not required but rather the matrix product $[H_e]^{-1}[T_e]$, this product is readily determined in an efficient manner by solving a system of equations with multiple right–hand–side vectors. Results obtained to–date indicate that the symbolic implementation of AQ4 (called ES24/A4S1) executes approximately twice as fast as the numerically integrated original version (ES8/AQ4).

Extensions to Linear Buckling and Free Vibration – The original formulation of the AQ4 shell element did not address the problems of linear buckling or free vibration. To address these problems, the formulation is extended and required the development of the geometric stiffness matrix and the consistent mass matrix. The geometric stiffness matrix is based on the membrane stress resultant prebuckling stress state and the nonlinear Green–Lagrange membrane strains. The geometric stiffness matrix is evaluated using Gauss quadrature after the integrand of each entry is evaluated symbolically using MAPLE. Numerical integration is required for the geometric stiffness matrix for the case of general quadrilateral elements wherein the Jacobian is a function of the natural coordinates of the element. As such, the integrand involves ratios of polynomials and cannot be easily integrated symbolically. The mass matrix is a consistent mass matrix and includes the effects of rotary inertia. The integrand of the mass matrix involves only polynomials of the natural coordinates and as such can be easily integrated symbolically using MAPLE.

Performance of this element for problems involving linear buckling and free vibration are reported by Rengarajan (1993). Comparison with other 4–node shell elements in COMET (4_ANS, 4_HYB, 4_STG) indicate that the AQ4 shell element formulation is substantially better both for buckling and vibration of flat and curved structures.

Beam Element Research

The work related to the beam element is to develop an AQ4–compatible 2–node beam element based on the Hellinger–Reissner variational principle. A 2–node assumed–stress hybrid 3–D beam element was installed as element processor ES22 in COMET using the generic element processor. Three areas of research were investigated: (i) development of the beam element; (ii) use of symbolic computations to accelerate the element computations; and (iii) extensions to linear buckling and free vibration analyses. The basic results for each area will now be summarized.

Development of Beam Element – Based on the Hellinger–Reissner variational principle, a 2–node assumed–stress hybrid 3–D beam was developed. The element has six degrees of freedom per node (3 translations and 3 rotations) plus six independent stress parameters. The effects of transverse shear deformation and rotary inertia are included in the formulation; however, the effects of cross–sectional warping are neglected. The beam element is implemented as element processor ES22 in COMET. Details of the formulation, implementation and testing of this element is reported by Deshpande (1993). Performance of this beam element for linear stress analysis is compared to that of the beam element in processor ES6/E210 – namely the STAGS 210 C^1 2–node beam element. In general, the two elements give comparable results for thin slender beams whether straight or curved. However; as the span–to–thickness ratio decreases, the new element provides a significant improvement in solution since the effects of transverse shear deformation are included in the formulation.

Use of Symbolic Computations – Similar to the shell elements, assumed–stress hybrid beam elements are usually associated with higher computational cost due to the fact that a matrix inverse is needed in the evaluation of certain element matrices. For example, the element stiffness matrix for the ES22/ABS2 beam element is a 12×12 matrix that is computed as followed:

$$[k_e]_{12\times12} = [T_e]^T[H_e]^{-1}[T_e]$$

where

$$[H_e]_{6\times6} = \int_{L_e} [P]^T[D][P]dx$$

$$[T_e]_{6\times12} = \int_{L_e} [P]^T[L][N]dx$$

The matrix $[D]$ is the compliance matrix from the strain–stress relations; the matrix $[L]$ is the linear differential operator matrix from the strain–displacement relations; the matrix $[P]$ is the matrix of stress field approximations; and the matrix $[N]$ is the matrix of displacement field approximations or shape functions. The need to invert the matrix $[H_e]$ for each element and to evaluate two integrals along the length of the element significantly increases the element computation time. In this research, symbolic computations using the MAPLE software system are used to evaluate the two integrals exactly. Explicit symbolic expressions for $[H_e]$ inverse were obtained in terms of the adjoint and determinant of $[H_e]$ since this matrix is only a 6×6 matrix. This complete symbolic form of the element is implement as element ABS2 in element processor ES22. In order to assess, a version of the beam element was developed (ES22/ABN2) which evaluates the integrals symbolically and determines the matrix product $[H_e]^{-1}[T_e]$ by solving a system of equations with multiple right–hand–side vectors. It was determined that the numerical evaluation of the matrix product is approximately 5% faster than the approach using a symbolic form of the matrix inverse and then a matrix–matrix multiply. This is due in part to the complexity of the FORTRAN expressions for the symbolic forms of the adjoint and determinant of $[H_e]$.

For the 4–node shell element, the symbolic evaluation of $[H_e]^{-1}$ is not possible because the symbolic expressions become unwieldy for a 24x24 matrix. However, since the explicit inverse is not required but rather the matrix product $[H_e]^{-1}[T_e]$, this product is readily determined in an efficient manner by solving a system of equations with multiple right–hand–side vectors. The "cost" of using this advanced multi–field element has been assessed and compared with other 4–node elements implemented in COMET. Significant computational savings have been accrued by using a combination of symbolic integration procedures and numerical analysis routines. These results are reported in a paper published in Communications in Numerical Methods for Engineering.

Extensions to Linear Buckling and Free Vibration – The formulation of the beam element was extended to linear buckling and free vibration analyses and required the development of the geometric stiffness matrix and the consistent mass matrix. The geometric stiffness matrix is based on the axial force resultant prebuckling stress state and the nonlinear

Green–Lagrange axial strain. The geometric stiffness matrix is evaluated symbolically using MAPLE. The mass matrix is a consistent mass matrix and includes the effects of rotary inertia. The integrand of the mass matrix is also easily integrated symbolically using MAPLE.

Performance of this element for problems involving linear buckling and free vibration are reported by Deshpande (1993). Comparison with the ES6/E210 2–node beam element in COMET indicate that the ES22/ABN2 beam element formulation does require more elements for convergence of higher modes and that convergence is to a lower value since transverse shear deformation and rotary inertia effects are included in the ES22/ABN2 formulation. Also the span–to–thickness ratio decreases, the new element provides a significant improvement in solution accuracy for linear buckling and free vibration problems.

SECOND–YEAR PROGRESS REPORT

This grant represents a continuation of the research effort initiated by the principal investigator while at Clemson University under NASA Grant No. NAG–1–1374. After the principal investigator relocated to the Old Dominion University, the research effort was renewed and initiated at ODU under NASA Grant No. NAG–1–1505 in April 1993. As such, this research thrust has been underway for approximately two years (one year at Clemson University and one year at ODU). Progress under this phase of the grant was reported in an oral presentation to the Computational Mechanics Branch at NASA Langley Research Center on June 30, 1994. Copies of the presentation material were given to NASA at that time.

The research effort has focussed primarily on completing a more thorough assessment of the assumed stress hybrid formulation by examining different assumed stress fields, on deriving diagonal mass coefficients for the beam and quadrilateral shell elements, and for preparing to move into the area of geometric nonlinear response prediction. Specific research objectives for the second year (first year at ODU) were as followed:

- Extend the 2–node assumed–stress hybrid beam element to handle geometrically nonlinear problems using both low–order and high–order corotation approaches.
- Validate the combined use of the assumed–stress hybrid 1–D and 2–D elements for modeling built–up structures.
- Extend the 2–D assumed–stress hybrid shell elements to handle geometrically nonlinear problems using both low–order and high–order corotation approaches.
- Develop a compatible 3–node assumed–stress hybrid shell element with drilling degrees of freedom with capabilities for linear stress, buckling and vibration analyses.

- Examine the drilling freedom formulations based on Allman–type shape functions and on the unsymmetric stress tensor.

Element Research

The first activity was to re–formulate the beam and shell elements to use the GCP or Generic Constitutive Processor for the constitutive matrix. Previously, the processor LAU was used for the shell element, and the processor LAUB was used for the beam element. The GCP uses the same format as processor LAU for shell elements, but a different convention than LAUB for the beam element. This required a complete re–derivation of the beam element kernel routines followed by an extensive period of testing and validation. At present, the shell element can handle any composite laminate and accommodates shear correction factors as implemented by the GCP. The beam element expects the GCP to provide the constitutive stiffness terms typically called EA, EI, and GJ. The beam element processor can handle any type of beam (isotropic or laminated) provided that the stiffness terms can be defined using the GCP.

The second activity was to develop and implement a diagonal mass matrix for the beam element. This was performed using the Hinton–Rock–Zienkiewicz approach. Options are now provided for either a consistent mass matrix or a lumped diagonal mass matrix. Free vibration test cases were performed and reported in Mr. W. Scott Carron's master's thesis (Carron, 1995).

The third activity was to investigate the stress recovery procedure for these elements. Since these elements are assumed stress–hybrid elements, the stress parameters can be computed and saved for each element or recovered from the element nodal displacements. As such, the element stresses (actually stress resultants) can be computed anywhere in the element accurately without differentiating the element nodal displacement field. However, it does require either storing or re–computing certain element terms during the solution process. As an alternative approach, a stress recovery procedure was investigated in which the element strains are computed by differentiating the nodal shape functions for the displacements – basically discarding the assumed–stress functions. The numerical results reported in Carron's thesis (Carron, 1995) indicate that the stress recovery procedure based on the assumed stress field was always better than that obtained by differentiating the nodal displacements. This came as no surprise, but served as a good example of a side benefit of these elements (improved displacement solutions and accurate stress recovery).

Table 1. Family of assumed–stress hybrid shell elements.

Element Name	Additional Modifications	Number of displacement dof		Number of Stress Parameters	
		Inplane	Out–of–Plane	Membrane	Bending
A4S1	Symbolic Version of AQ4	12	12	9	13
A4S2	Modified Membrane Stress Field	12	12	11	13
A4S3	Bubble functions for out–of–plane only	12	15	9	17
A4S4	Bubble functions for inplane only	14	12	11	13
A4S5	Bubble functions for both	14	15	11	17
A4S6	Bubble functions for out–of–plane only	12	15	9	19

Use of Bubble Functions

The finite element approximations for the 4–node element can be expected to improve by adding degrees of freedom at the center of the element. The contribution of these degrees of freedom should not affect the edges of the elements. One such approximation is called a "bubble function" which has a value of unity at the element center in the natural coordinate frame and zero along all edges of the element. Addition of the bubble function for the translational and bending rotation degrees of freedom are considered independently and require modification of the stress approximations. These modifications led to the development of a family of assumed–stress hybrid shell elements with drilling degrees of freedom denoted as A4S*i* where *i* ranges from 1 to 6. The features of these elements are summarized in Table 1.

The performance of each element of this family was assessed for linear stress analysis only. The results indicate that overall the A4S1 element is very robust and accurate. Elements A4S2 and A4S4 are also quite good but increase the element–level computations and did not show any improvement over the performance of the A4S1 element. The remaining elements (A4S3, A4S5, and A4S6) appear to be quite stiff and sensitive to extreme

Table 2. Performance of elements using the MacNeal–Harder cantilever beam.

A : Extension, B : In-plane Shear, C : Out-of-plane Shear, D : Twist									
Load	4_ANS	4_MSC	4_STG	A4S1	A4S2	A4S3	A4S4	A4S5	A4S6
Rectangular-Shaped Elements									
A	0.995	0.995	0.994	0.998	0.998	0.998	0.988	0.988	0.988
B	0.904	0.904*	0.915	0.993	0.993	0.993	0.993	0.993	0.993
C	0.980	0.986	0.986	0.981	0.981	0.981	0.981	0.981	0.981
D	0.856	0.941	0.680	1.009	1.009	1.009	1.009	1.009	0.858
Trapezoidal-Shaped Elements									
A	0.761	0.996	0.991	0.998	0.998	0.998	0.998	0.998	0.998
B	0.305	0.071*	0.813	0.986	0.985	0.986	0.986	0.986	0.986
C	0.763	0.968	†	0.969	0.969	0.968	0.969	0.968	0.961
D	0.843	0.951	†	1.007	1.007	1.004	1.007	1.004	0.856
Parallelogram-Shaped Elements									
A	0.966	0.996	9.989	0.998	0.998	0.998	0.998	0.998	0.998
B	0.324	0.080*	0.794	0.977	0.972	0.977	0.977	0.977	0.977
C	0.939	0.977	0.991	0.980	0.980	0.980	0.980	0.980	0.979
D	0.798	0.945	0.677	1.007	1.007	0.999	1.007	0.999	0.846

* Q4S results for these cases are 0.993, 0.988, and 0.986, respectively.

† Produces a singular stiffness matrix.

mesh distortion. The assessment of different assumed stress fields and the performance of the element for linear stress, buckling, and free vibration analyses has been completed and is reported in a paper in the International Journal for Numerical Methods in Engineering. As a result, future work is directed only towards the A4S1 element formulation.

Drilling Freedoms

In first–order shear deformation plate theory, the kinematic relations involve three translations and two bending rotations – the rotation normal to the plate surface, the so–called drilling rotation does not enter the kinematic relations. Hence at an element level, the drilling degree of freedom is not present; however, at the global or assembled level, the degrees of freedom associated with the structure include the drilling rotation. While assembling the element stiffness matrices to form the global stiffness matrix, if the elements connected to a particular node happen to be coplanar, then the drilling rotation of the node is not resisted and the global stiffness matrix is singular. This singularity could be avoided if the drilling degree of freedom is included at the element level. Generally the drilling degrees of freedom are suppressed at the beginning of an analysis since they do not enter the kinematic description of the problem. There have been numerous attempts in formulating elements with drilling degrees of freedom. Two main approaches have been success-

ful. One approach is to introduce the drilling rotations in the functional as independent variables, while the second approach is to introduce the drilling rotations in the finite element displacement approximations.

In the first approach, the true drilling or inplane rotation is defined in terms of the skew–symmetric part of the displacement gradient as

$$\theta_z = \frac{1}{2}\left(\frac{\partial v}{\partial x} - \frac{\partial u}{\partial y}\right)$$

Reissner (1965) presented a mixed variational principle in which this definition of the inplane rotation was relaxed and then later enforced in the variational statement as a constraint through the use of Lagrange multipliers. On imposing the stationary conditions on the functional, the Lagrange multipliers were identified as the skew–symmetric part of the stress tensor. Reissner's formulation introduced the drilling rotation independent of the inplane displacements. Hughes and Brezzi (1989) have shown that Reissner's mixed formulation holds good in a continuous case, but becomes unstable if discrete approximations of the continuous space is made using standard interpolation functions. They modified Reissner's functional to include an additional term which stabilizes the function in discrete approximations. Ibrahimbegovic, Taylor, and Wilson (1990) used the Hughes and Brezzi formulation to develop a quadrilateral membrane element using independent interpolation fields for rotations and Allman–type shape functions for the inplane displacements. Later Ibrahimbegovic and Wilson (1991) developed triangular and quadrilateral flat shell elements along the same lines. The drilling rotations which occur in Allman–type shape functions are not true drilling rotations rather they are more like *rotational connectors* (Aminpour, 1990). Hence Iura and Atluri (1992) argue that in using Allman–type shape functions compatibility will not be satisfied directly along nodal lines of the shell element. They have developed an element where the rotations are interpolated from the true drilling rotations evaluated from the skew–symmetric part of the displacement gradient at the nodes. These issues are still unresolved.

In the second approach, the drilling rotation was introduced through the inplane displacement field approximations (e.g., Allman, 1984; Bergan and Felippa, 1985). Allman (1984) used a quadratic function for the normal component of the displacement and a linear function for the tangential component of the displacement along each edge of the element. Cook (1986) noted that the same shape functions can be derived by eliminating the translational displacements at the midpoint of an edge in favor of the corner drilling rotations. He applied it to an 8–node quadrilateral membrane element to obtain a 4–node quadrilateral

element. Soon other investigators followed suit including the work of Aminpour (1990) which was based on an assumed–stress hybrid formulation. These elements have been shown to be quite robust for linear stress analysis problems – particularly for membrane problems. The present work involves extensions of the work of Aminpour (1990) to assess linear buckling, free vibration and geometrical nonlinearities.

Application Studies

Skewed Laminated Plate – Buckling of a skewed laminated plate subjected to combined axial compression and inplane shear was studied to consider the performance of the A4S1 (new AQ4) element for buckling analysis of a composite structure with skewed elements. The plate is skewed by 45°, the laminate is a $[\pm 45/90/0]_s$ laminate, and a 31×31 mesh of nodes is used to compute the reference solution. This mesh and a contour plot of the transverse deflection component of the buckling mode shape are shown in Figure 1. Convergence of the buckling coefficient as a function of the number of nodes along each edge of the plate is shown in Figure 2 for two sets of boundary conditions (i.e., all edges clamped and all edges simply support). In both cases, the present A4S1 element converges quickly and correlates well with the solution obtained using the STAGS shell element named 4_STG.

Pear–Shaped Cylinder – Linear stress and buckling analyses were performed on the pear–shaped cylinder shown in Figure 3. It has a uniform thickness and is simply supported. Only one–quarter of the cylinder is modeled, and the loading is uniform end shortening. This noncircular cylindrical shell problem poses certain difficulties due to the changes in curvature around the shell. Comparison of the transverse deflection normalized by the shell thickness as a function of the circumferential coordinate is shown in Figure 4. Results are obtained using both the 4ANS element and the A4S1 (new AQ4) element. These results are in very good agreement. Linear buckling analyses were also carried out on this cylinder, and good correlation with reference solution was obtained. The buckling modes for the lowest two modes are shown in Figure 5. The buckling loads are normalized by the buckling loads obtained using the 9ANS element and a 7×51 mesh (i.e., 4.393 and 6.483, respectively).

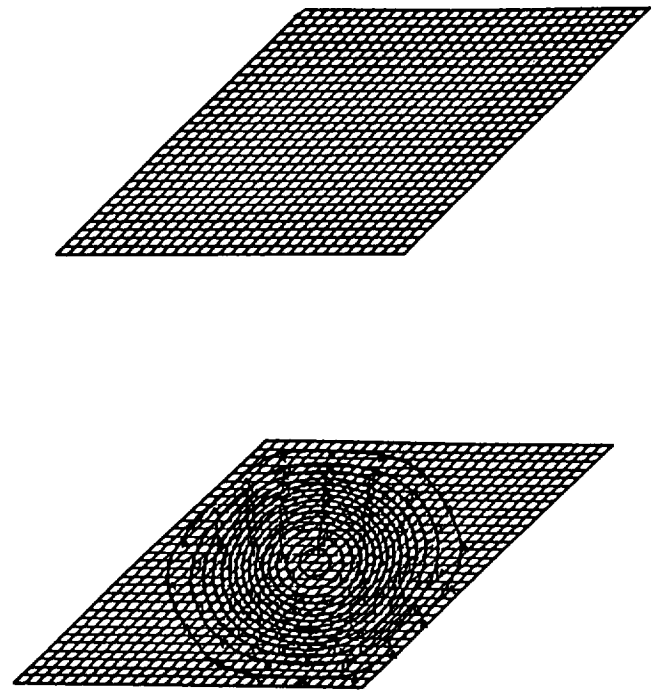

Figure 1. Refined finite element mesh and buckling mode shape contour plot.

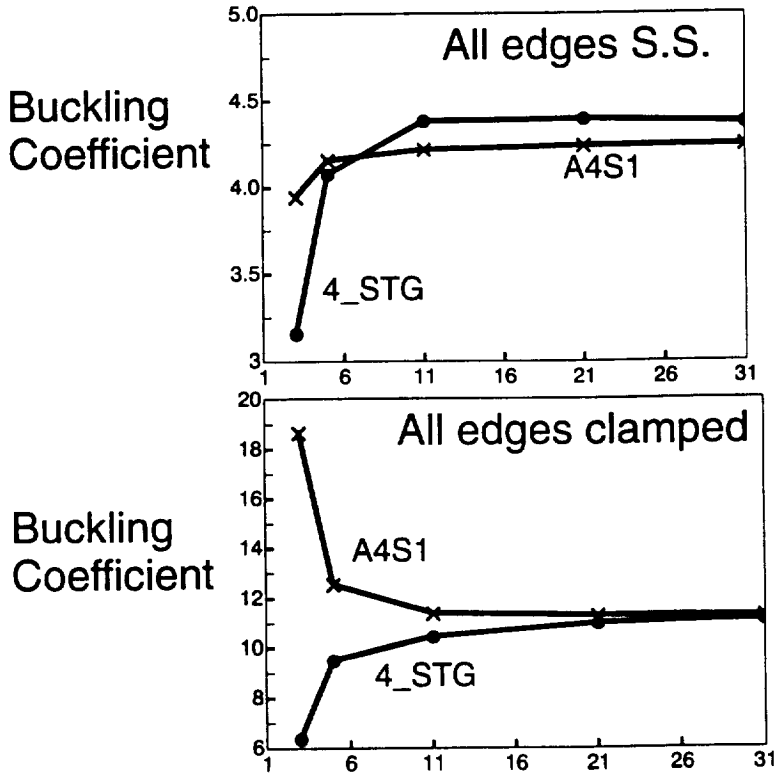

Figure 2. Convergence of the buckling coefficient.

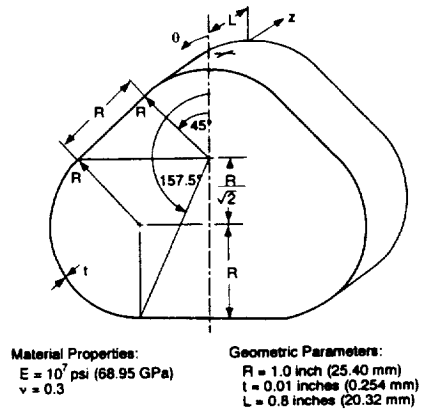

Figure 3. Pear–shaped cylinder: geometry and material properties.

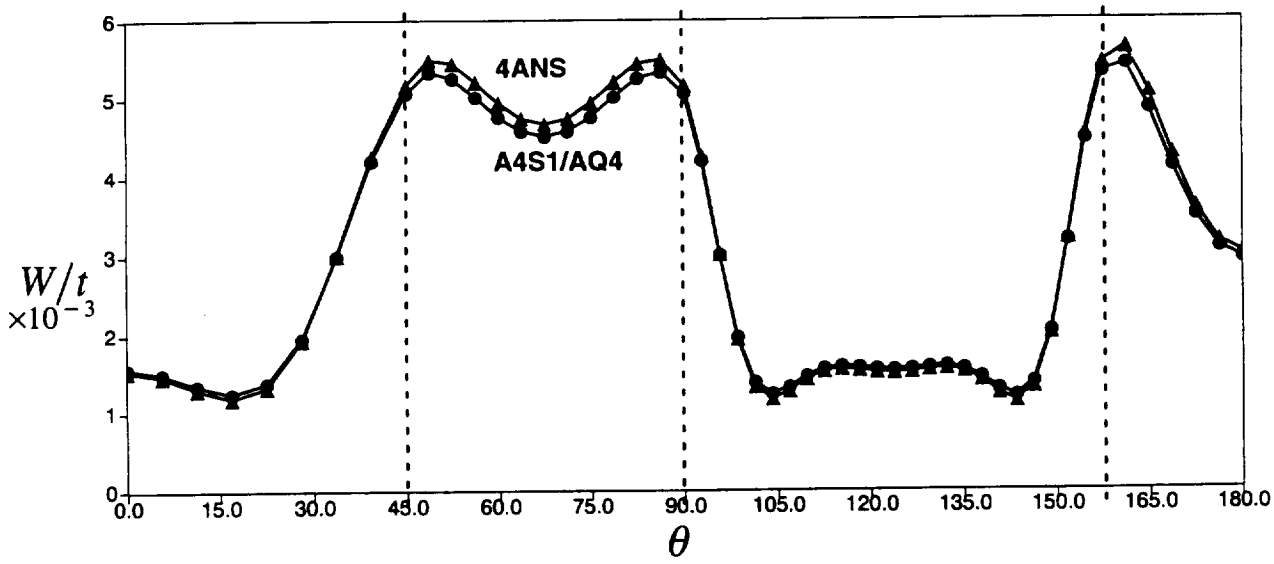

Figure 4. Comparison of transverse deflection distribution around the shell.

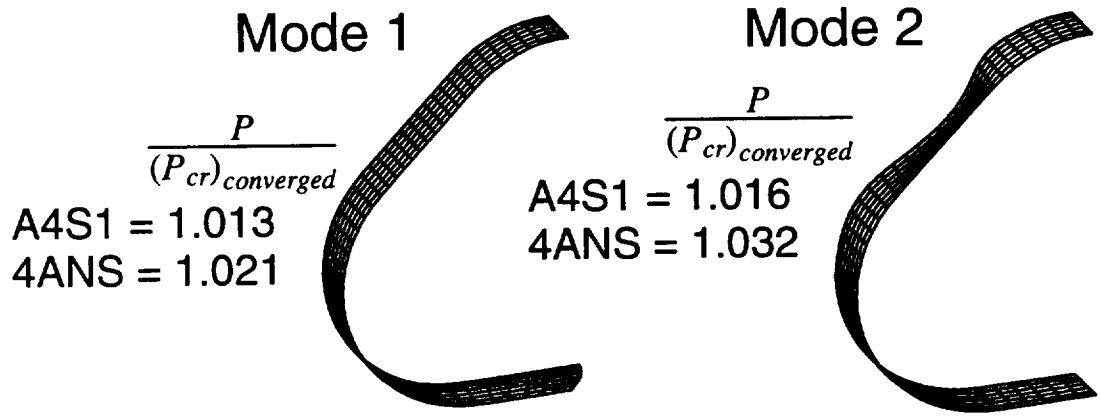

Figure 5. Comparison of linear buckling analysis results.

Circular Cylindrical Shell – To assess the eigenvalue analysis capability of the AQ4 shell element, linear buckling and vibration analyses were carried out on an elastic isotropic thin circular cylinder. The cylinder is simply supported at both ends and has an R/t ratio of 100. The geometric stiffness matrix and the consistent mass matrix used in these computations are formed symbolically and then implemented into COMET using the GEP. In the analysis, a one–eighth symmetric model is used; however, for visualizing the eigenmode shapes, a full cylinder is considered.

Comparison of the buckling results using the 4–node shell elements in COMET is given Rengarajan (1993). The buckling mode shape is shown in Figure 6(a). These finite element results are compared with the theoretical solution and indicate that the ES24/A4S1 or AQ4 element produces significantly better results than the other elements for the same discretization due in part to the assumed–stress field features of the element. For the coarse mesh, the use of the STAGS 410 element (ES5/E410) resulted in triggering a "mechanism" in the mode shape.

Comparison of the vibration results using the 4–node shell elements is given Rengarajan (1993). These results indicate that the AQ4 element produces better results than the other shear–flexible elements due in part to the higher–order assumed–displacement field by including the drilling freedoms. The AQ4 assumed–displacement field is still of lower order than the STAGS element which neglects transverse shear effects. The vibration mode shape corresponding to the lowest vibration frequency is shown in Figure 6(b).

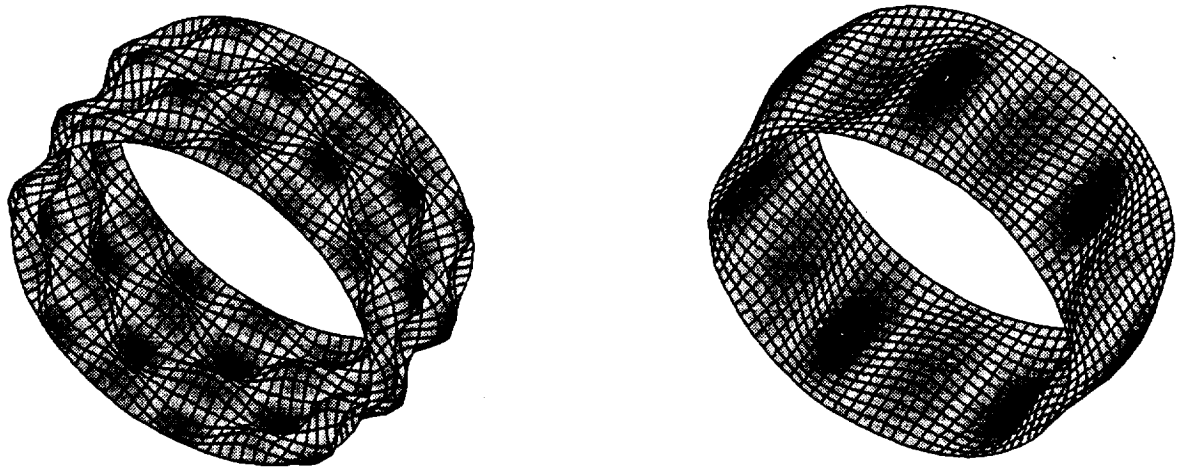

(a) Buckling mode shape

(b) Vibration Mode Shape.

Figure 6. Eigenmode shapes.

Grumman Shear Panel – Another assessment problem was associated with a large finite element model of a shear buckling problem of interest to Grumman Aerospace Corporation. A significant amount of time was allocated to applying the beam and quadrilateral shell elements to this NASA–customer application problem – Grumman shear buckling composite panel. The original analysis was carried out by Dr. Larry Sobel of Grumman using the Grumman version of STAGS and then using the STAGS elements in COMET. Difficulties were encountered by Dr. Sobel in performing the COMET analysis. These new COMET results did not correlate with his existing STAGS results, and it was unclear whether the difficulties were associated with the STAGS–element implementation in COMET, the nonlinear analysis procedure, or some other modeling issues. Eventually, an implementation error associated with the sign of the twisting moment was detected in the STAGS shell element kernel routines implemented in COMET as processor ES5.

However, when the Grumman composite shear panel was analyzed using the elements developed under this research grant, linear stress and buckling results were obtained that matched both other analytical results as well as results obtained from experiment. This complex model involved a combination of the 2–node beam and 4–node shell elements in a single finite element model and demonstrate their combined use in large finite element simulations.

Nonlinear Analysis Procedure

Next steps were taken to validate the nonlinear solution procedure available in COMET's CLAMP procedure `nl_static_1`. Solution to small test problems appeared to be readily obtained and accurate. However, application to NASA finite element models of large stiffened composite panels led to convergence problems in the postbuckled region of the response. Numerous test cases and example problems were analyzed; yet the same convergence difficulties could not be duplicated except with the large model. This large model had many complicating features including multi–point constraints. A definitive resolution to this problem was not found; however, issues related to the modeling strategy were raised and were to be considered by the NASA engineers. Even though this activity consumed a large amount of time and produced little direct benefit for the research thrust of the grant, it did provide a thorough assessment of the nonlinear solution procedure and its performance which is an integral part of the research. The nonlinear analysis procedure has now been thoroughly tested and several improvements made. A tutorial presentation on the nonlinear solution procedure was given to personnel from the Computational Mechanics Branch on January 6, 1995 following a grant review presentation that same day.

The basic strategy for extending the assumed–stress hybrid beam and shell elements to handle geometric nonlinearities is through the use of the Generic Element Processor (or GEP) of COMET. The GEP provides a variety of utilities including both those for constitutive modeling (namely, the Generic Constitutive Processor or GCP) and those for large arbitrary rotations (namely, the corotation utilities). By using the corotational utilities, these elements will be extended to problems involving geometric nonlinearities by two approaches. The first approach is the low–order corotation approach that involves linear strain–displacement relations at the element level and the large displacement/rotation capability at the global level through the corotation utilities. This is accomplished by formulating and implementing the internal force vector for this family of elements in addition to the capabilities provided under NASA Grant No. NAG–1–1374. The low–order corotation approach is straightforward for the beam element since the drilling degrees of freedom are actual degrees of freedom that enter the formulation through the kinematics of the problem. However, this approach has not been demonstrated for plate and shell elements with drilling degrees of freedom.

The second approach is the high–order corotation approach that involves nonlinear strain–displacement relations at the element level and the large displacement/rotation capability at the global level through the corotation utilities. In this case, the internal force vector and material stiffness matrix will need to be formulated in order to account for the nonlinear strain–displacement relations and implemented. The high–order corotational approach and the total Lagrangian approach for assumed–stress hybrid elements poses some challenges that will increase the computational effort at the element level – similar to that of displacement–based elements.

Adaptive Dynamic Relaxation Supplement

A supplement to the grant enabled an exploratory study of the adaptive dynamic relaxation algorithm for three–dimension hyperelastic nonlinear structures on massively parallel processing (MPP) systems. This method exploits the advantages of explicit time integration for both static and transient dynamic analyses of structures. The ADR algorithm is described in a three–part paper published in the international journal for Computer Methods in Applied Mechanics and Engineering. The algorithm has been shown to be very scalable as the number of processors increases, has minimal memory requirements for each processor, and minimizes the interprocessor communication. For example, on the Intel Touchstone Delta MPP system with 512 processors, a relative speed–up of 386 was obtained. Results from this study are summarized in a paper published in the International Journal for Numerical Methods in Engineering.

Interface Element Supplement

Upon the hiring of Dr. Mohammad A. Aminpour by ODU in January 1994, a supplement task was initiated under this grant related to interface element technology. This task allowed Dr. Aminpour to begin his research upon arrival at ODU. Dr. Aminpour reported on this aspect of the work independently.

THIRD–YEAR PROGRESS REPORT

This grant represents a continuation of the research effort initiated by the principal investigator at Old Dominion University under NASA Grant No. NAG–1–1505 which was renewed in May 1994. The activity continued until May 1995 and then was extended to December 31, 1995 under a no–cost extension. As such, this research thrust has been underway for approximately three years (one year at Clemson University and two years at ODU). Progress under this phase of the grant was reported in two oral presentations to the Computational Mechanics Branch at NASA Langley Research Center on January 6, 1995 and on December 12, 1995. Copies of the presentation material were given to NASA at the time of presentation.

Specific research objectives for the third year (second year at ODU) were as followed:

- Extend the 2–node assumed–stress hybrid beam element to handle geometrically nonlinear problems using both low–order and high–order corotation approaches.
- Extend the 2–D assumed–stress hybrid shell elements to handle geometrically nonlinear problems using both low–order and high–order corotation approaches.
- Validate the combined use of the assumed–stress hybrid 1–D and 2–D elements for modeling built–up structures.
- Develop a compatible 3–node assumed–stress hybrid shell element with drilling degrees of freedom with capabilities for linear stress, buckling and vibration analyses.

Element Research

The element research performed during this period focussed on the extensions needed for geometrically nonlinear analysis for both the shell and beam elements. The approach taken was to exploit the corotational utilities and and existing element subroutines. To do this, only the internal force vector needed to be computed and used along with the linear material stiffness matrix and the geometric stiffness matrix. The internal force vector is computed

as

$$\{ f_{int} \} = \int_A [N]^T [\mathcal{L}]^T \{\sigma^*\} \, dA = [T]^T \{\beta\}$$

This form is readily available since the matrix [T] is computed for the linear material stiffness matrix and the vector of unknown stress parameters {β} are computed at the element level.

In the preceding approach, the local element strain–displacement relations involve only the linear terms and the the nonlinear behavior is treated through the corotational formulation. In the corotational formulation, a local element coordinate system is established and element deformations are measure relative to the local system which corotates with the element through the global coordinate system. This approach is called low–order corotation. This approach works well provided that local element rotations are small. Typically results can be improved by refining the mesh which essentially adds more corotating coordinate systems.

As an alternative, the local element strain–displacement relations could include the nonlinear terms as well as the linear terms. In so doing, each element would be able to treat large local rotations than in the low–order corotational formulation before refining the mesh would be necessary. However, this high–order corotational formulation for the assumed–stress hybrid elements requires the solution of a nonlinear system at the element level which significant increases the computational cost of the element. Presently, an assessment of the low–order corotational formulation for nonlinear analysis using the new beam and shell elements indicates that implementing the nonlinear strain–displacement relations at the element level is not needed.

Application Studies

Many applications have been analyzed during this phase of the research. The applications studies involving the beam element are given by Carron (1995). Only two beam problems are considered herein: 45–degree circular bend problem and the clamped–hinged deep circular arch. The application studies involving the shell element are given here for selected applications although many more have been studied to insure the reliability of the element and its implementation. Three shell problems are considered: the elastica problem, the hinged–free cylindrical panel, and the Raasch challenge problem. The final application problem involved a model of the HSCT using the AQ4 element for its 4–node quadrilateral elements.

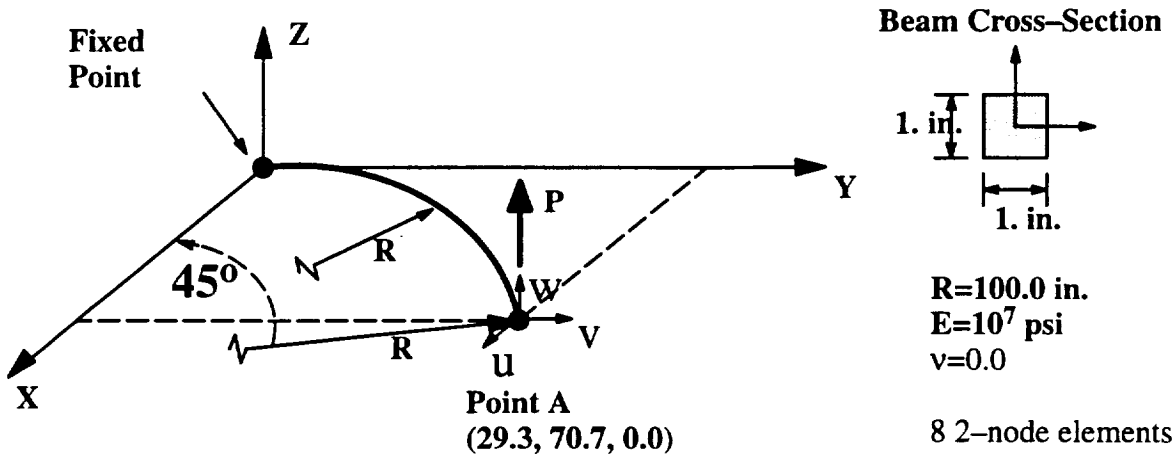

Figure 7. 45–Degree Circular Bend: Geometry and Properties.

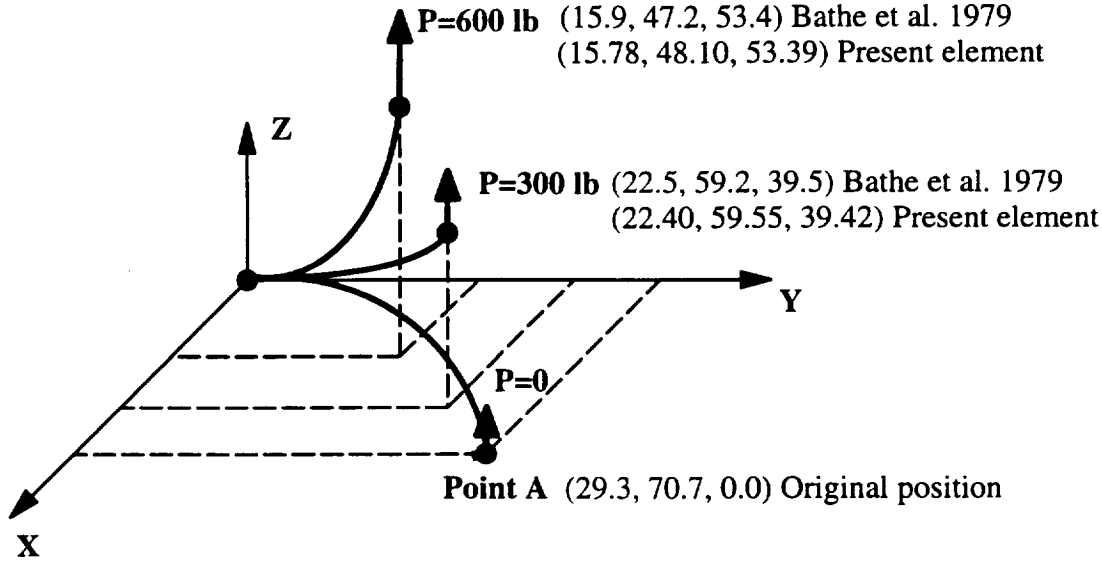

Figure 8. Deformed Shapes and Results Comparisons.

45–degree Circular Bend Problem – The 45–degree circular bend problem shown in Figure 7 is a severe test of the corotational approach and the 2–node beam element because of the three–dimensional aspects of the deformation process. The beam is originally in the X–Y plane and is pulled in the Z direction. The finite element model had only eight 2–node beam elements along the beam's length, and the low–order corotational approach is used. The results are shown graphically on Figure 8 for two values of load and compared with the solutions obtained by Bathe and Bolourchi (1979). The position of Point A in the XYZ coordinate system from Bathe and Bolourchi (1979) is compared with the position obtained using the present 2–node element, and the results are quite good. Comparison to other investigators is given by Carron (1995).

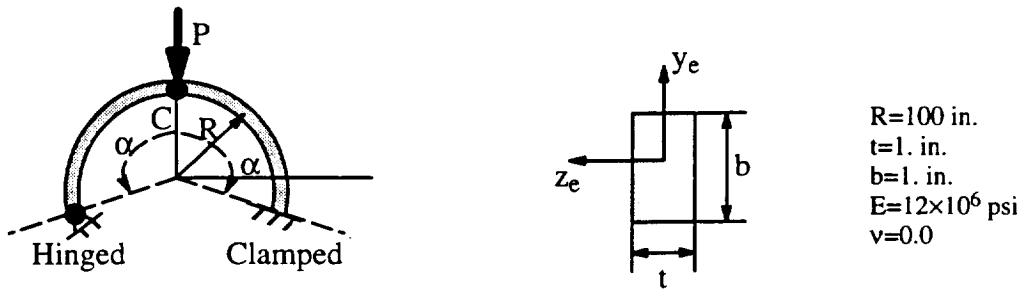

Figure 9. Clamped–hinged circular arch.

Clamped–hinged Circular Arch problem – The circular arches considered herein have the same geometry as those studied by DaDeppo and Schmidt (1975) and shown in Figure 9. The following notation is used: P is the downward concentrated point load acting at the crown of the arch at Point C; 2α is the subtending angle of the arch; R is the centroidal radius of curvature; E is the modulus of elasticity; ν is Poisson's ratio; I is the moment of inertia; U is the horizontal deflection of the crown point C; and V is the vertical deflection of the crown point C. The rectangular cross–sectional dimensions and elastic modulus are selected such that $EI = 10^6$ lb–in.^{2} Two sets of boundary conditions are considered. One set is asymmetric and are different at the two ends of the arch (one is clamped; the other is hinged), while the other set is symmetric with both ends being clamped. In both cases, the applied load P at the arch crown (at Point C) is normalized such that $\overline{P} = PR^2/EI$. The most common geometry considered by other researchers is the case for a subtending angle 2α of 215° and asymmetric boundary conditions. This geometry corresponds to a deep circular arch. The solutions obtained by DaDeppo and Schmidt (1975) are based on Euler's nonlinear theory of an inextensible elastica with no restrictions on the magnitude of the deflections. For this subtending angle, the normalized collapse load $\overline{P}_{cr}$ from DaDeppo and Schmidt (1975) is 8.97. Numerical solutions are obtained using the present element with the low–order corotational formulation and the modified Newton–Raphson solution procedure with arc–length control.

The load versus deflection curves obtained for the 20–element model are shown in Figure 10 and compared with the analytical solutions of DaDeppo and Schmidt (1975). The normalized applied load $\overline{P}$ is shown as a function of the vertical deflection V and the horizontal deflection U at Point C normalized by the centroidal radius of the arch R. These results clearly indicate the accuracy of the present element and the solution approach. Also shown in Figure 8 are the results obtained from a linear analysis which indicate the unconservative nature of such a prediction for nonlinear softening systems.

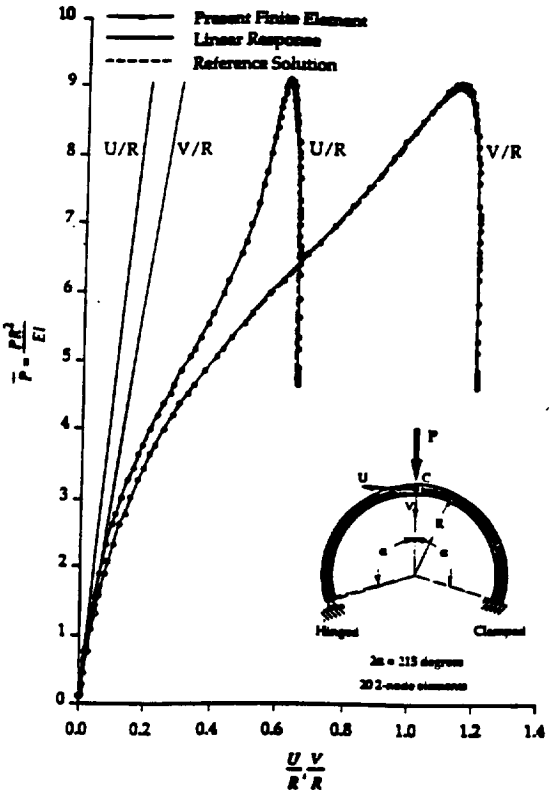

Figure 10. Load vs. deflections for clamped–hinged deep circular arch (2α=215°).

Using the 20–element model, the subtending angle 2α is varied to determine its effect on the structural behavior of such elastic circular arches. Results of this parametric study along with the analytical solutions obtained by DaDeppo and Schmidt (1975) are presented in Figure 11. The solutions obtained using the present element are in good agreement with the reference solutions. As the subtending angle increases, a *cusp* in the collapse load versus subtending angle curve shown in Figure 11 occurs at approximately 2α=210°. On either side of this cusp, a smooth curve appears to describe the structural behavior.

Examining the deformed geometries for arches with different subtending angles 2α on either side of the cusp reveals different structural behavior. For 2α=120°, the arch exhibits a prominent local bending behavior near the arch crown. The arch does not *wrap* around the hinged support and yet continues to snap through. For 2α=260°, the arch exhibits minor local bending near the crown. However, the arch does exhibit a strong tendency to *wrap* around the hinged support in an asymmetric sidesway mode. For 2α=215°, the arch exhibits behavior that is more complex. As the load increases from zero, the arch deforms under local bending for a load level well below the collapse load. Just prior to reaching the collapse load, the asymmetry of the arch boundary conditions, as well as a local bending re-

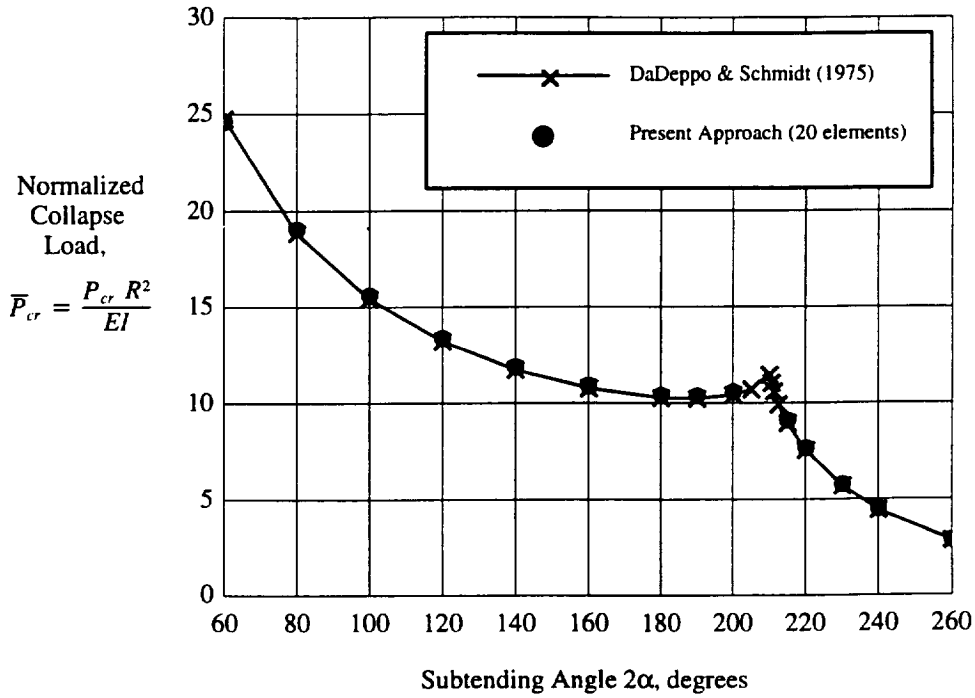

Figure 11. Collapse load versus subtending angle for clamped–hinged circular arch.

sponse or buckle near the crown, begin to be amplified. Near the collapse load, the arch begins to *wrap* around the hinged support.

Several observations were made based on these studies reported by Carron (1995). First, as the value of the subtending angle increases, the slope of these load versus deflection curves prior to collapse tends to increase. Also as the angle increases, the value of the collapse load decreases except for values near the cusp in Figure 11. Near the cusp, the load–deflection curve exhibits a rapid increase in stiffness as the collapse load is approached. For arches with a subtending angle greater than 210°, the nonlinear results indicate that, after very large pre–collapse deflections (when the crown has deflected vertically to the level of the supports), no further increase in the horizontal deflection U at the crown occurs.

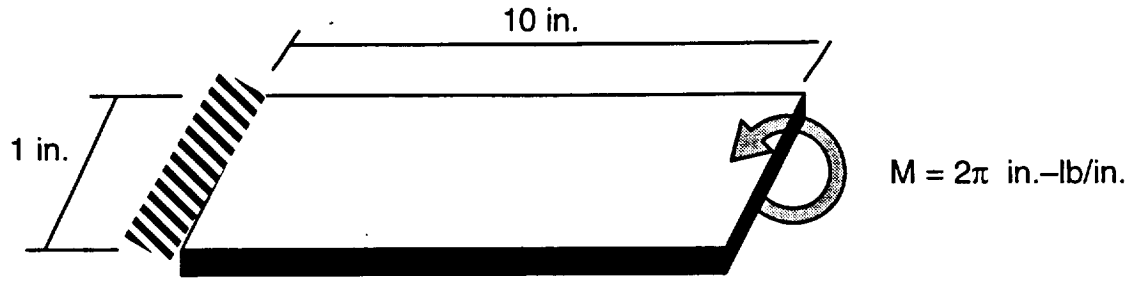

E=120 psi; ν=0.3; thickness, t=1.0 in.

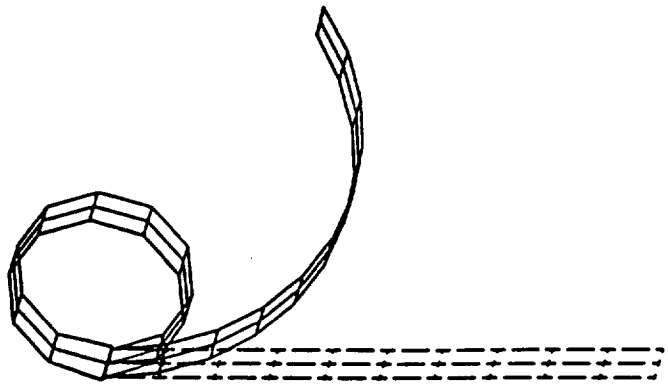

Figure 12. Elastica Problem: geometry, material properties, and loading.

Elastica Problem – The elastica problem is solved as another nonlinear problem with large deflections and rotations. The geometry, material properties and loading are shown in Figure 12. The nonlinear elastic response of this cantilevered beam bent into a circle by an applied end moment as shown in Figure 12 is characterized by the moment versus end deflection response shown in Figure 13. The response is described in terms of the applied moment and the end deflection. a vertical tangent is approached as the end deflection approaches 1.2 times the beam length. Three solutions are presented in Figure 11. The reference solution is taken as the solution obtained using a 5×1 mesh of 9–node ANS elements (ES1/EX97). Solutions were also obtained using 4–node shell elements with a 10×2 mesh using the 4–node ANS element and the AQ4 element. All results are essentially the same through the loading range considered.

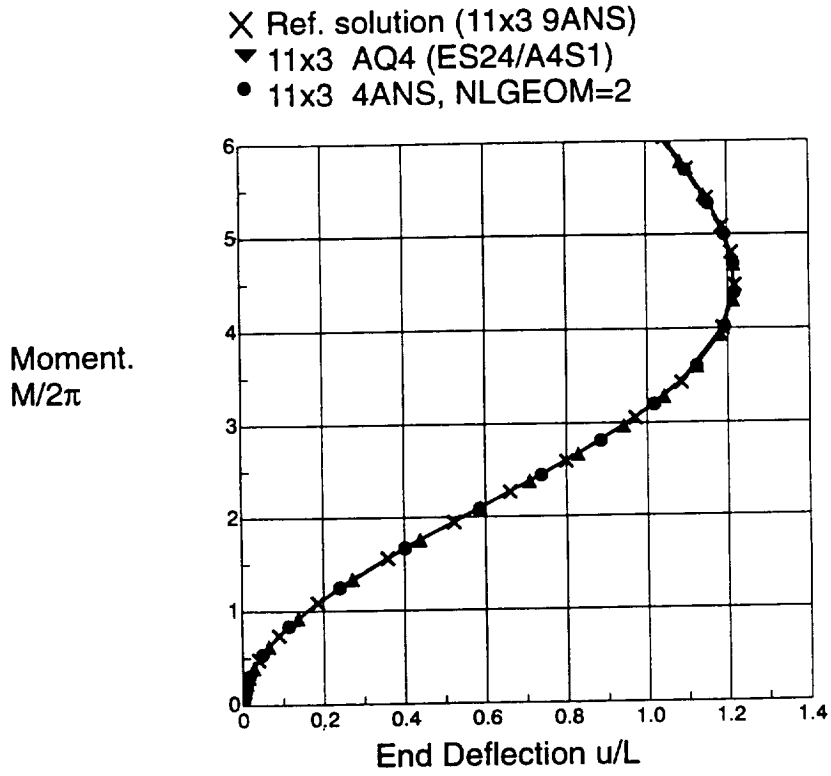

Figure 13. Elastica Problem with an End Moment: Moment vs. End Deflection.

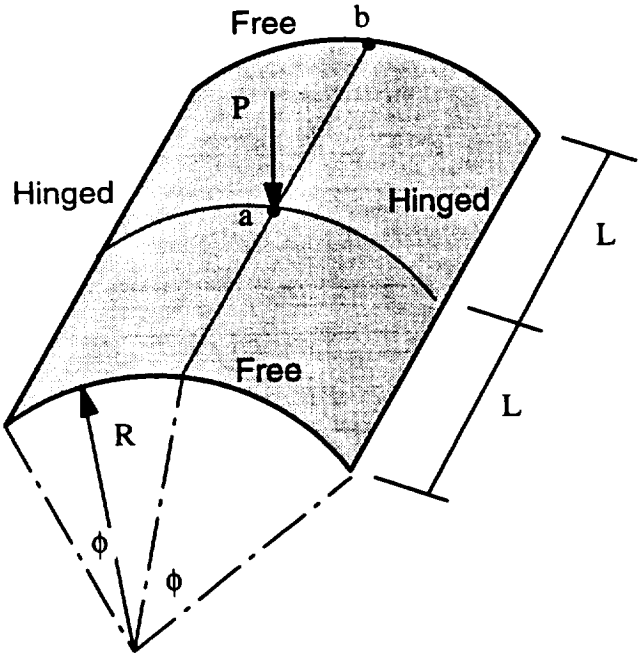

R=2540 mm
L=254 mm
thickness, t=6.35 mm
R/t=400

E=3.10275 kN/mm^2
ν=0.3
ϕ=0.1 radians

Figure 14. Hinged–free cylindrical panel: geometry, material properties and loading.

Hinged–Free Cylindrical Panel – The hinged–free cylindrical panel subjected to a center transverse point load is considered to validate the nonlinear aspects of the AQ4 shell element based on the low–order corotational formulation. This structure is shown in Figure 14. The structural response exhibits a limit point, a snap–through behavior, and a snap–back behavior.

The nonlinear response of the panel is shown in Figure 15 for a midpoint on the free edge (Point b). Two meshes are considered, and the reference solution is taken to be that obtained using a 5×5 mesh of 9ANS elements. The results in Figure 15(a) indicate the response obtained using two meshes of the AQ4 element developed as part of this research. For both meshes, nearly the same nonlinear behavior is obtained. The only difference appears to be after the shell's free edge has snapped through to an inverted position. The results in Figure 15(b) indicate the response obtained using a 5×5 mesh of 4ANS elements with both the low–order and high–order corotational formulation (i.e., NLGEOM=1 and NLGEOM=2, respectively). These results appear to bracket the reference solution.

The nonlinear response of the panel is also shown in Figure 16 for the center point (Point a). Two meshes are considered, and the reference solution is taken to be that obtained using a 5×5 mesh of 9ANS elements.The results in Figure 16(a) indicate the response obtained using two meshes of the AQ4 element. For both meshes, nearly the same nonlinear behavior is obtained. Differences appear after the limit point as the snap–back response occurs. In this region of the nonlinear response, severe local changes in curvature occur and the 5×5 mesh of 4–node elements with the low–order corotation approach is not sufficient to reproduce the reference solution. Adding more elements (i.e., essentially adding more local reference frames) has the effect of refining the solution to obtain the reference solution. As an alternative, using the high–order corotational approach should have the same effect. The results in Figure 16(b) indicate the response obtained using a 5×5 mesh of 4ANS elements with both the low–order and high–order corotational formulation. These results are similar to the reference solution up until snap–back occurs. The two solutions exhibit a different character than anticipate from previous results.

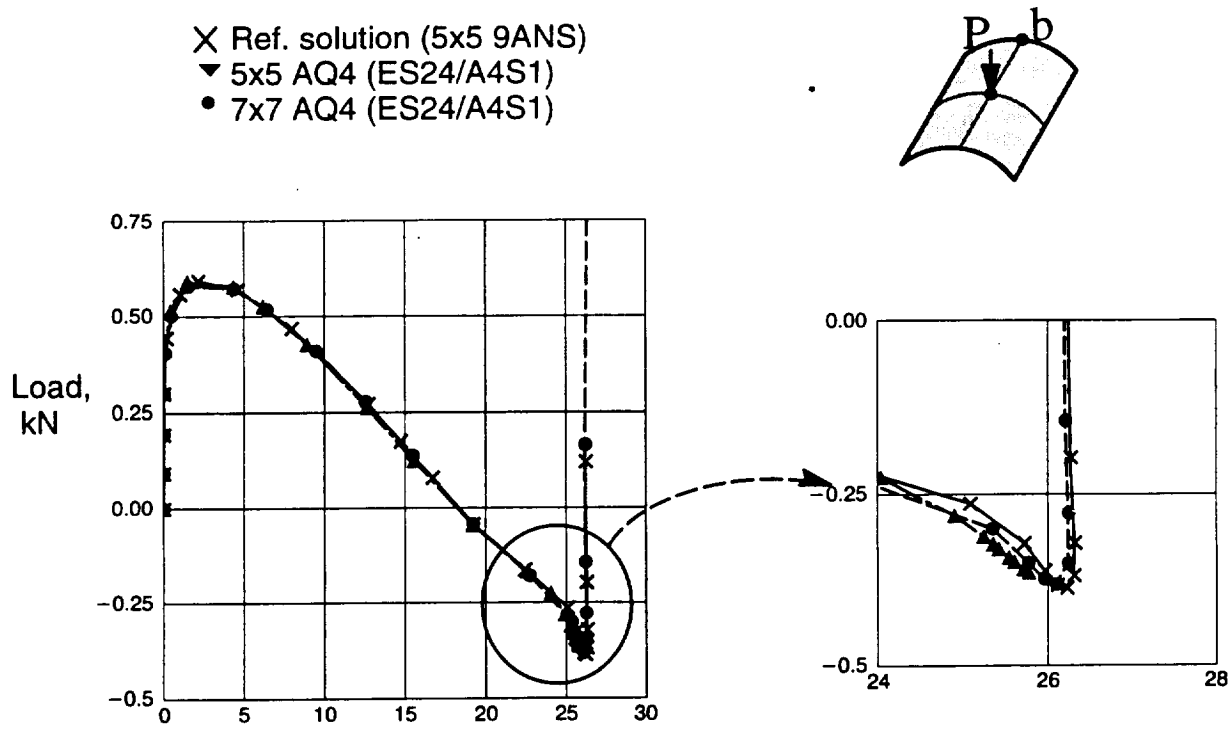

(a) AQ4 results.

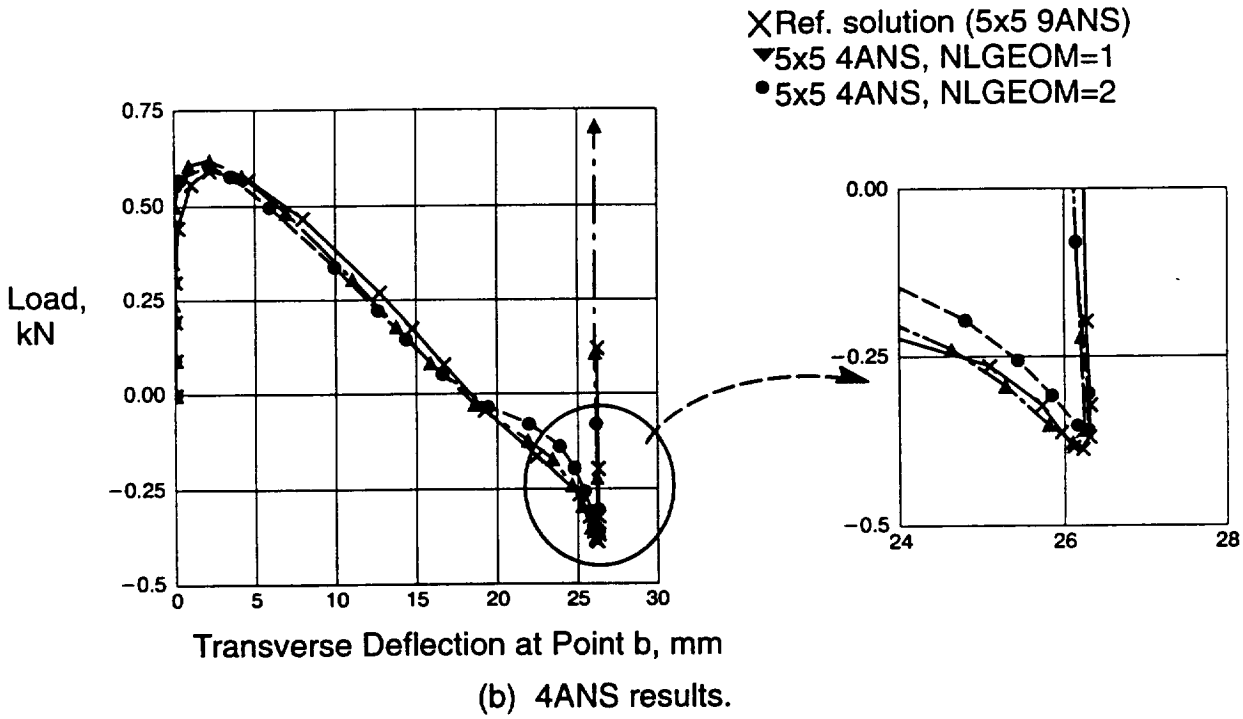

(b) 4ANS results.

Figure 15. Hinged Cylinder: Load vs. Free Edge Point Deflection

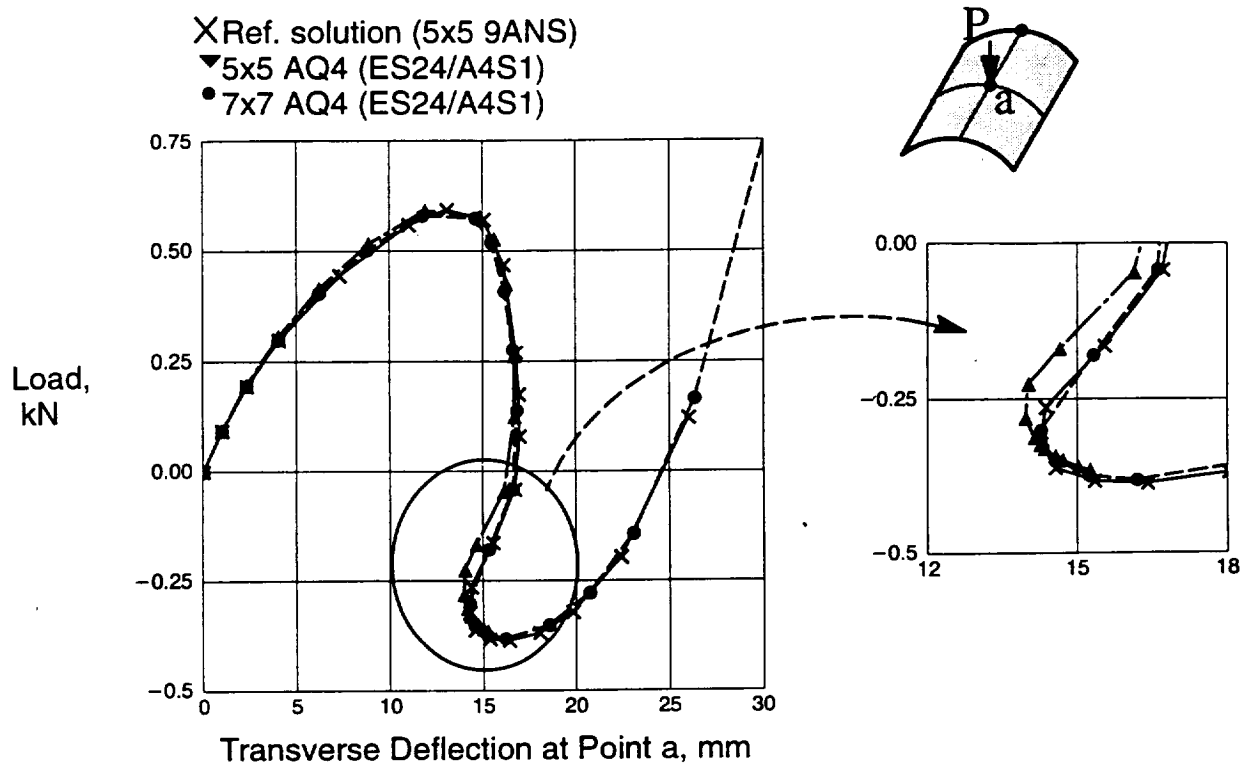

(a) AQ4 results.

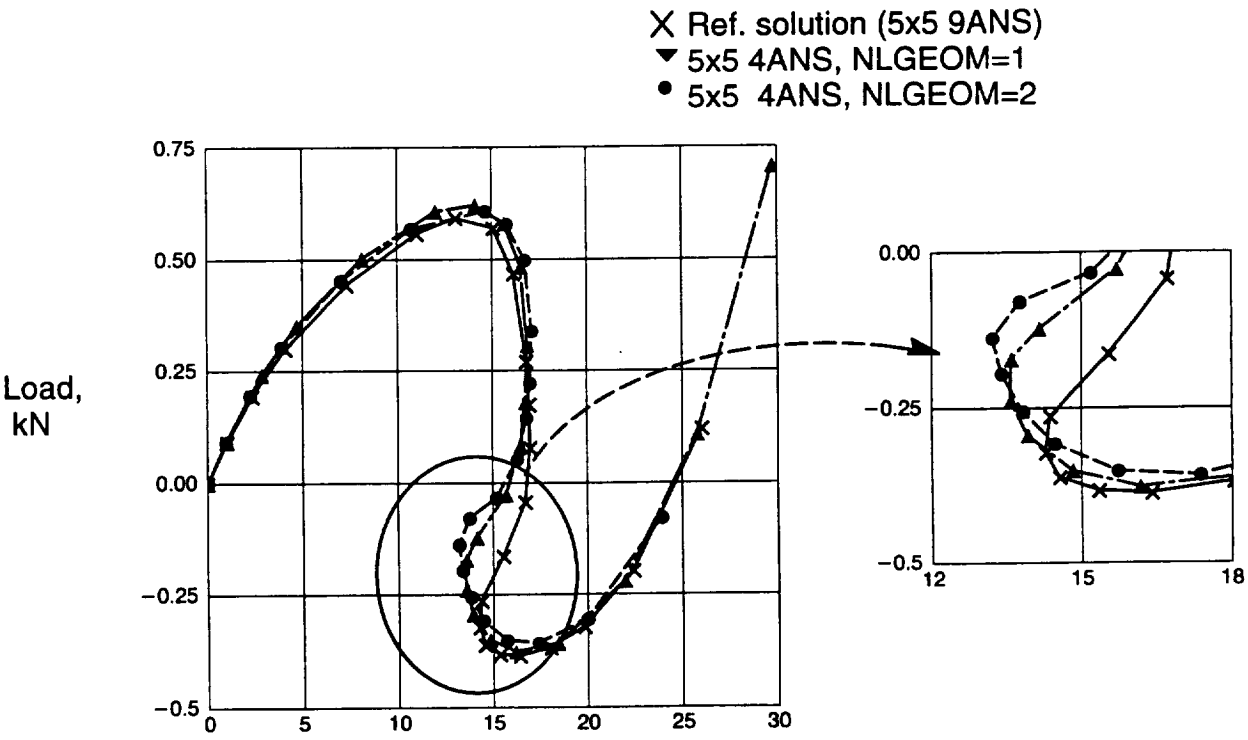

(b) 4ANS results.

Figure 16. Hinged Cylinder: Load vs. Center Point Deflection

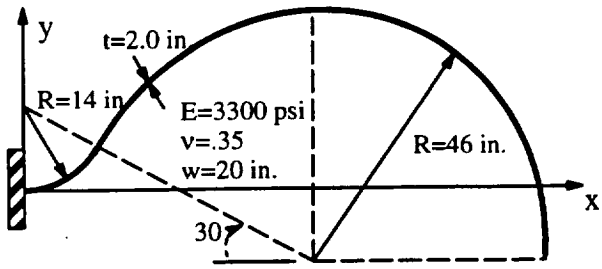

Figure 17. Geometry of the Raasch challenge problem.

Raasch Challenge Problem – The Raasch Challenge problem grew out of a presentation at the Structures Technical Forum at the 1990 MSC World Users' Conference. The geometry is essentially that of a "hook" as shown in Figure 17. The hook is a thick curved strip clamped at one end (all degrees of freedom constrained to zero) and loaded by a unit in–plane shear load in the width (or *z*) direction at the other end. In this paper, the unit shear load is treated as a uniformly distributed shear load of 0.05 lb/in. (total shear force of 1.0 lb). The hook has essentially two different curved segments that are tangent at their point of intersection. One segment spans an opening angle of 60–degrees and has a radius of 14 inches. The second segment spans an opening angle of 150–degrees and has a radius of 46 inches. Both segments have a thickness *t* of 2.0 inches and a width *w* of 20 inches (aspect ratio *w/t* equal to 10 – limit for first–order, shear–deformation theory). The hook material is isotropic with an elastic modulus of 3300 psi and a Poisson's ratio of 0.35.

Early MSC/NASTRAN results by Harder (1991) for this problem indicated that as the mesh of QUAD4 elements was refined, the solution did not converge unless the transverse shear flexibility (controlled by the parameter MID3) was suppressed. Recommendations to users at that time were to suppress the transverse shear flexibility (set MID3=0 on the PSHELL card) and also to suppress the drilling freedoms caused by the facet shell geometry approximations (used a large value for the artificial stiffness parameter K6ROT). The MSC element developers then proceeded to developed the QUADR element which included a drilling freedom at each node and also created the unique surface normal option for the low–order shell elements in order to resolve this behavior and to improve element performance of their low–order quadrilateral elements over that reported by MacNeal and Harder (1985).

At the 1995 MSC World Users' Conference, Hoff et al. (1995) presented new results for this problem using both the QUAD4 and QUADR shell elements from MSC/NASTRAN Version 68.2. The QUAD4 element is a 4–node flat, quadrilateral, displacement–based shell ele-

ment without any drilling freedoms. The QUADR element is related to the QUAD4 and includes drilling freedoms at the nodes. Both shell elements can accommodate transverse shear flexibility. These new results also indicate that as the mesh is refined, the solution does not converge for either shell element unless the transverse shear flexibility is suppressed. The addition of drilling freedoms to the element formulation (i.e., the QUADR element) did provide some improvement in the element performance, but the solutions obtained using successively refined meshes still did not converge. The value of the tip deflection in the direction of the load obtained for the most refined mesh using the QUADR element was still more than twice their reported converged value (given as 5.012 inches by Hoff et al., 1995) and represents an improvement over the value obtained with the QUAD4 element which was nearly five time the converged value. Results were also presented using a new surface normal option (SNORM parameter) which activates the creation of unique grid point normals for adjacent shell elements. Details of this option were not presented by Hoff et al. (1995). With surface normals active and transverse shear flexibility suppressed, the solutions obtained without and with nodal drilling freedoms (QUAD4 and QUADR elements, respectively) are essentially the same and exhibit rapid convergence. In addition, the solutions obtained with surface normals active and also transverse shear flexibility included converge rapidly to their reference solution for both elements which corresponds to a value approximately 5% more flexible than that obtained with transverse shear flexibility suppressed. Hoff et al. (1995) concluded that unique surface normals at grid points are needed to improve the element performance of the MSC low–order quadrilaterals.

The results for various spatial discretizations and different shell elements shown in Figure 18 are given in Table 3 wherein the isotropic properties of the material are used. That is, the transverse shear moduli are equal to the in–plane shear modulus (i.e., $G_{13} = G_{23} = G_{12} = \frac{E}{2(1+\nu)}$). The reference value for the tip deflection used herein is 4.9352 inches obtained using a refined 20×136×2 mesh of 8 node, assumed–stress hybrid solid brick elements (8_HYB). This value represents a 1.6% stiffer solution than that given by Hoff et al. (1995). In all shell element models, the `auto_dof_sup` option is true, and the option `auto_triad` is false. The shell elements which neglect transverse shear flexibilities (4_STG, 3_DKT) converge to a solution that is slightly stiffer than the solution obtained using a refined mesh of three–dimensional solid elements. This behavior indicates that transverse shear flexibilities can at most account for only 5% of the tip deflection. However, the solutions obtained with elements which do account for transverse shear flexibilities do not converge as the mesh is refined. The MIN3 and AQ4 elements give somewhat better solu-

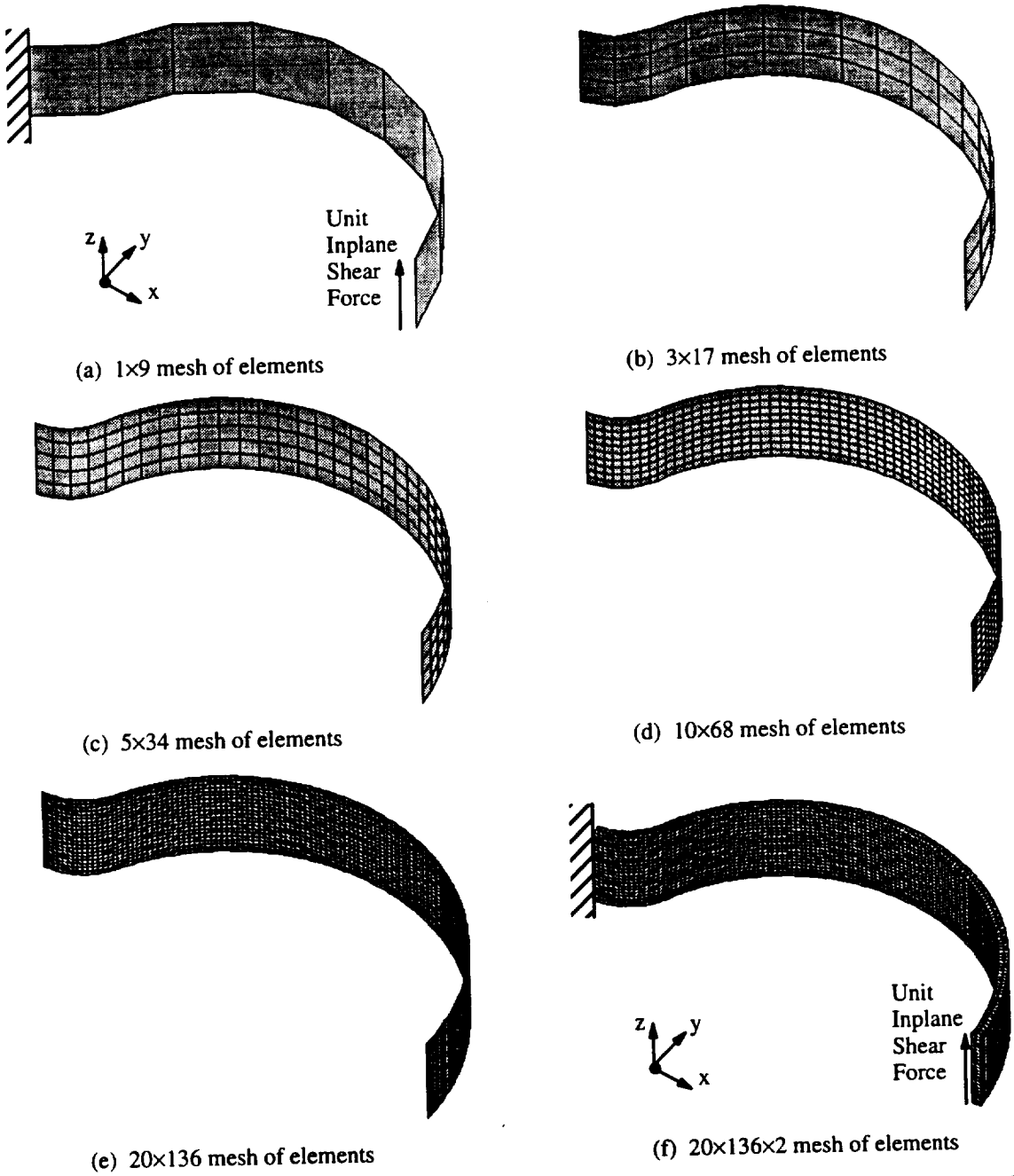

(a) 1×9 mesh of elements

(b) 3×17 mesh of elements

(c) 5×34 mesh of elements

(d) 10×68 mesh of elements

(e) 20×136 mesh of elements

(f) 20×136×2 mesh of elements

Figure 18. Two–dimensional 4–node shell quadrilateral finite element models considered and three–dimensional 8–node brick finite element model used as reference solution.

tions than the 4_ANS and 4_HYB elements but still predict more than twice the tip deflection of the three–dimensional solution for the most refined mesh. The MIN3 element suppresses all drilling freedoms at the element level (artificial drilling stiffness), while the AQ4 element includes the drilling freedoms to improve the in–plane displacement field approximations. By including the drilling freedoms, the approximation for the in–plane displacement field component normal to an element edge is raised from linear to quadratic along that edge. Shell elements without transverse shear flexibility in COMET (4_STG and 3_DKT) appear to converge to an appropriate value (i.e., 5% stiffer than the three–dimensional solution). Shell elements with transverse shear flexibility do not appear to converge. Surface normals or new computational nodal triads influence the results obtained using COMET but not as successfully as reported by Hoff et al. (1995). If the hook is made thin, then all shell elements tested converge

Table 3. Curved Hook Results for In–plane Shear Loading

Mesh of Elements $n_w \times n_L$	Normalized Tip Deflection in Direction of Load							
	Element Type							
	4_ANS	4_STG	AQ4	4_HYB	MIN3	3_DKT	8_HEX	8_HYB
1×9	0.9411	0.9061	1.1382	1.1562	1.0666	0.8481	0.5041	0.6922
3×17	1.0335	0.9398	1.0375	1.1678	1.1341	0.9323	0.8136	0.9432
5×34	1.2559	0.9512	1.1064	1.3858	1.2588	0.9478	0.9275	0.9738
10×68	2.0618	0.9541	1.3492	2.1767	1.6357	0.9532	0.9736	0.9890
20×136	4.8111	0.9548	2.2529	4.9045	2.7760	0.9479	0.9932	1.0000
Results are normalized by solution obtained using a 20×136×2 mesh of 8 node, assumed–stress hybrid solid brick elements (8_HYB): 4.9352 for w/t=10. `auto_dof_sup=true; auto_triad=false`								

Boeing HSCT Model – As a large–scale application study, a finite element model of the High Speed Civil Transport (HSCT) was analyzed using these elements. The analysis model and cases are company proprietary and specifics are not available. Ms. Tina Lotts of AS&M under contract for the Computational Mechanics Branch made these analysis runs and provided the normalized results shown in Table 4. The results are normalized by the results obtained by using MSC/NASTRAN as the finite element system.

Table 4. HSCT Results for Various Load Cases

Load Case	COMET ES5/E410	COMET ES24/A4S1
1	1.0692	1.1183
2	1.0333	1.1142
3	0.9823	1.0000
4	0.9755	0.9895
5	1.0112	1.0128
7	1.0038	1.0199
8	0.9830	0.9830
9	1.0075	1.0262
10	0.9823	1.0000

RESEARCH PRODUCTS

Under NASA Grants NAG–1–1374 at Clemson University and NAG–1–1505 at Old Dominion University, the following research products have been developed. The element research was facilitated by the use of the COMET software system and in particular the Generic Element Processor or GEP. Two element processors were developed: ES22 for the 2–node beam element and ES24 for the 4–node quadrilateral shell element. These processors have been transferred to NASA and are included in the baseline version of COMET. Three master's and one doctoral students completed their degree requirements with full or partial support from this grant. Three conference papers and six journal papers have been published related to work sponsored by this grant with two additional papers still under review. Copies of each thesis or dissertation and each conference paper or journal article have already been given to the technical monitor.

Software

- Processor ES22 – three–dimensional elastic beam element for linear stress, buckling, free vibration, and geometric nonlinear analysis using the low–order corotational formulation.
- Processor ES24 – two–dimensional elastic quadrilateral shell element for linear stress, buckling, free vibration, and geometric nonlinear analysis using the low–order corotational formulation.

Grant Review Presentations

- May 28, 1992
- June 30, 1994
- January 6, 1995
- December 12, 1995

Graduate Students

- Govind Rengarajan, "Assumed–Stress Hybrid Shell Elements with Drilling Degrees of Freedom," Clemson University, August 1993, MS in Engineering Mechanics.
- V. R. Deshpande, "Development of an Assumed–Stress Hybrid C^0 Beam Element," Clemson University, August 1993, MS in Engineering Mechanics.
- David R. Oakley, "Concurrent Adaptive Dynamic Relaxation Algorithm for Nonlinear Hyperelastic Structures," Clemson University, May 1994, PhD in Engineering Mechanics.
- W. Scott Carron, "Assumed–Stress Hybrid Beam Element for Nonlinear Elastic Stress Analysis," Old Dominion University, May 1995, MS in Aerospace Engineering.

Conference Papers and Presentations

- Oakley, D. R. and Knight, N. F., Jr. "Nonlinear Structural Response using Adaptive Dynamic Relaxation on a Massively Parallel Processing System," Proceedings of the Fifth Conference on Nonlinear Vibrations, Stability, and Dynamics of Structures, June 12–16, 1994, VPI&SU, Blacksburg, VA.
- Carron, W. S., "Sfatic Collapse of Circular Arches," Presented at the 1995 AIAA Mid–Atlantic Regional Student Conference, April 1995,NASA Langley Research Center (Second Place Winner based on written paper and oral presentation).
- Knight, N. F., Jr., "The Raasch Challenge for Shell Elements," AIAA Paper No. 96–1369. Proceedings of the 37th AIAA/ASME/ASCE/AHS/ASC Structures, Structural Dynamics, and Materials Conference, Salt Lake City, UT, April 15–17, 1996, pp. 450–460.
- Knight, N. F., Jr. and Carron, W. S., "Static Collapse of Elastic Circular Arches," AIAA Paper No. 96–1648. Proceedings of the 37th AIAA/ASME/ASCE/AHS/ASC Structures, Structural Dynamics, and Materials Conference, Salt Lake City, UT, April 15–17, 1996, pp. 1374–1383.

Journal Papers

- Rengarajan, G., Aminpour, M. A., and Knight, N. F., Jr., "Improved Assumed–Stress Hybrid Shell Element with Drilling Degrees of Freedom for Linear Stress, Buckling, and Free Vibration Analyses," *International Journal for Numerical Methods in Engineering,* Vol. 38, No. 11, 1995, pp. 1917–1943.
- Rengarajan,G., Knight, Jr., N. F., and Aminpour, M. A., "Comparison of Symbolic and Numerical Integration Methods for an Assumed–Stress Hybrid Shell Element," *Communications in Numerical Methods in Engineering*, Vol. 11, No. 4, April 1995, pp. 307–316.
- Oakley, D. R., and Knight, N. F., Jr., "Adaptive Dynamic Relaxation Algorithm for Nonlinear Hyperelastic Structures: Part I. Formulation," *Computer Methods in Applied Mechanics and Engineering,* Vol. 126, 1995, pp. 67–89.
- Oakley, D. R., and Knight, N. F., Jr., "Adaptive Dynamic Relaxation Algorithm for Nonlinear Hyperelastic Structures: Part II. Single–Processor Implementation," *Computer Methods in Applied Mechanics and Engineering,* Vol. 126, 1995, pp. 91–109.
- Oakley, D. R., Knight, N. F., Jr., and Warner, D. D. "Adaptive Dynamic Relaxation Algorithm for Nonlinear Hyperelastic Structures: Part III. Parallel Implementation," *Computer Methods in Applied Mechanics and Engineering,* Vol. 126, 1995, pp. 111–129.
- Oakley, D. R., and Knight, N. F., Jr., "Nonlinear Structural Response using Adaptive Dynamic Relaxation on a Massively–Parallel–Processing System," *International Journal for Numerical Methods in Engineering*, Vol. 39, No. 2, 1996, pp. 235–259.
- Knight, N. F., Jr., "The Raasch Challenge for Shell Elements," Submitted to *AIAA Journal*, February 1996.
- Knight, N. F., Jr. and Carron, W. S., "Static Collapse of Elastic Circular Arches," Submitted to *AIAA Journal*, February 1996.

CONCLUDING REMARKS

Assumed–stress hybrid beam and shell elements have been formulated, implemented, and tested. The implementation was performed in COMET using the generic element processor. The beam element is available in element processor ES22 while the shell elements are available in element processor ES24. Numerical results for each element indicate that both element types are accurate and robust. Excellent correlation with published solutions and/or exact analytical solutions has been demonstrated for flat and curved structures, for thick and thin structures, and for linear stress, buckling and free vibration problems. Extensions to geometrically nonlinear problems has been achieved for both the beam and shell element by using the low–order corotational formulation. Excellent results have been obtained in comparison to other published solutions for nonlinear problems. However, as the deformation mode becomes more complex, more and more elements are required to model the behavior accurately. For example, as the number of buckle halfwaves increases, the number of elements also increases due to the rapid change in the deformation mode. Augmenting the linear strain–displacement relations with the nonlinear terms may relieve this requirement; however, the computational effort at the element level will increase significantly.

REFERENCES

1. Aminpour, Mohammad A.: A 4–Node Assumed–Stress Hybrid Shell Element With Rotational Degrees of Freedom. NASA CR–4279, April 1990a.
2. Aminpour, Mohammad A.: Direct Formulation of a 4–Node Hybrid Shell Element With Rotational Degrees of Freedom. NASA CR–4282, April 1990b.
3. Bathe, K.–J.; and Bolourchi, S.: Large Displacement Analysis of Three–Dimensional Beam Structures. **International Journal for Numerical Methods in Engineering**, Vol. 14, 1979, pp. 961–986.
4. Carron, W. Scott: Assumed–Stress Hybrid Beam Element for Nonlinear Elastic Stress Analysis. Master's Thesis, Old Dominion University, May 1995
5. Char, B. W. ; Geddes, K. O.; Gonnet, G. H.; Leong, B. L.; Monagan, M. B.; and Watt, S. M.: **MAPLE V Library Reference Manual**. Springer–Verlag, New York, 1991.
6. DaDeppo, D. A.; and Schmidt, R.: Instability of Clamped–Hinged Circular Arches Subjected to a Point Load. **ASME Journal of Applied Mechanics**, Vol. 42, 1975, pp. 894–896.
7. Deshpande, Venkateshwar Rao: Development of an Assumed–Stress Hybrid C^0 Beam Element. Master's Thesis, Clemson University, 1993.

8. Harder, R. L.: "The Raasch Challenge," Presentation charts presented at the Structures Technical Forum at the 1991 MSC World Users' Conference (12 charts).

9. Hoff, C. C.; Harder, R. L.; Campbell, G.; MacNeal, R. H.; and Wilson, C. T.: Analysis of Shell Structures using MSC/NASTRAN's Shell Elements with Surface Normals. **Proceedings of the 1995 MSC World Users' Conference**, Universal City, CA, May 8–12, 1995, The MacNeal–Schwendler Corporation, Paper #26, 18 pages.

10. MacNeal, R. H.; and Harder, R. L.: A Proposed Standard Set of Problems to Test Finite Element Accuracy. **Finite Elements in Analysis and Design**, Vol. 1, 1985, pp. 3–20.

11. Oakley, David R.: Concurrent Adaptive Dynamic Relaxation Algorithm for Nonlinear Hyperelastic Structures. Doctoral Dissertation, Clemson University, May 1994.

12. Park, K. C.; and Stanley, G. M.: A Curved C^0 Shell element Based on Assumed Natural–Coordinate Strains. **ASME Journal of Applied Mechanics**, Vol. 108, pp. 278–290, 1986.

13. Rengarajan, Govindarajan: Assumed–Stress Hybrid Shell Elements with Drilling Degrees of Freedom. Master's Thesis, Clemson University, 1993.

14. Stanley, G. M.: Generic Element Processor: Application to Nonlinear Analysis. Proceedings of the NASA Workshop on Computational Structural Mechanics – 1987, Part 2. Nancy P. Sykes (editor), pp. 571–651, 1989.

15. Stanley G. M.; Park, K. C.; and Hughes, T. J. R.: Continuum Based Resultant Shell Elements. **Finite Element Methods for Plate and Shell Structures, Volume 1: Element Technology**. T. J. R. Hughes and E. Hinton (editors), Pineridge Press International, Swansea, pp. 1–45, 1986.

16. Stanley, G. M.; and Nour–Omid, S.: The Computational Structural Mechanics Testbed Generic Element Processor Manual. NASA CR–181728, March 1990.

17. Stewart, Caroline B. (Compiler): The Computational Structural Mechanics Testbed User's Manual. NASA TM–100644, October 1989.

18. Tessler, A.; and Hughes, T. J. R.: An Improved Treatment of Transverse Shear in the Mindlin–Type Four–Node Quadrilateral Element. **Computer Methods in Applied Mechanics and Engineering**, Vol. 39, pp. 311–335, 1983.